15

Geotechnical Study of Unstable Slopes: A Case Study at Sunkoshi Power-house Site, Central Nepal

G.S.Pokharel
Soil, Rock and Concrete Laboratory, Nepal Electricity Authority
Bhagwan Pau, Swayambhu, Kathmandu, Nepal

Nepal is a mountainous country with enormous hydropower potential. However, to construct the necessary infrastructure many geological problems need to be overcome, in particular problems of slope instability. Nowadays, these issues are addressed during the feasibility and design phases of a hydropower project. In the past, however, due attention was not given to geological issues when planning projects. This has led to problems that affect the smooth operation of many of the early hydropower projects, problems that now have to be faced by the Nepal Electricity Authority (NEA). A case study of such a project from central Nepal – the Sunkoshi power station – is presented here. The project, completed in 1971, suffers from problems caused by an unstable slope.

This paper considers the following aspects of the Sunkoshi project: the major natural hazards in the area; the geological conditions; geological investigations and studies carried out since 1977; Interpretation of the data acquired during monitoring; additional investigations and studies carried out since 1990; and conclusions about the condition of the unstable slope and recommendations for its long term stabilisation.

Introduction

Nepal is a mountainous country located in the central Himalayas and has an enormous potential for hydropower development. A number of hydropower projects have been constructed to harness this resource and many new hydropower projects are at various levels of planning or construction.

Every hydropower project in Nepal has to be located on sloping mountain terrain. Only the power-houses may be located on gentler slopes or in plains areas. Because of this, slope stability studies and studies of erosion processes in the slopes adjoining hydropower stations are a major consideration during the feasibility and engineering design stages of implementation. After the construction of a hydropower project in Nepal, a major part of the annual maintenance budget is spent on civil works to repair damage done by slope failures caused by natural disasters. The most common types of natural hazards are mass wasting processes such as landslides, mud and debris flows, and mud avalanches, debris torrents, and glacial lake outburst floods (GLOF).

Various natural disasters have already hydropower projects in Nepal. Larger ones include the following (those affecting the Sunkoshi are described in the next section).

- 1993 – landslides, floods, and debris flows caused enormous siltation in the Kulekhani reservoir, Makawanpur district, central Nepal, washed out the penstock over the Jurikhet Khola, destroyed the Kulekhani-II headworks, and increased the bed level of the Kali Khola at the tail water end of the Kulekhani-II powerhouse.
- 1985 – the Namche small hydropower station in Solu Khumbu district, eastern Nepal, was completely washed out by a GLOF before it was put into commission.

- 1994 – The headworks of the Achham small hydropower project were completely washed out by a large flood just before its completion.
- deposition of erosion sediment, although a less dramatic natural process, has had a significant impact on various hydropower schemes by silting up, and thus reducing the economic life, of the reservoirs.

The Sunkoshi Power Station

The Sunkoshi Power Station is a run of the river type of power plant located on the Sunkoshi River in Sindhupalchowk district (Figure 15.1). The plant was completed in 1971and handed over to the Nepal Electricity Corporation. It lies four hours drive east of Nepal's capital, Kathmandu. This power station has been damaged by natural hazards several times. Even before it was built it was known that the area was prone to such events. In 1935 an outburst of the Taraco glacial lake in Tibet destroyed a large area of cultivated land in the Bhotekoshi basin (the Bhotekoshi is a major tributary of the Sunkhoshi which it joins about 700m downstream of the Bhotekoshi bridge at Barhabishe). In 1964 an outburst of the Zhanzangho glacial lake in Tibet caused an 8m rise in the water level in the Bhotekoshi.

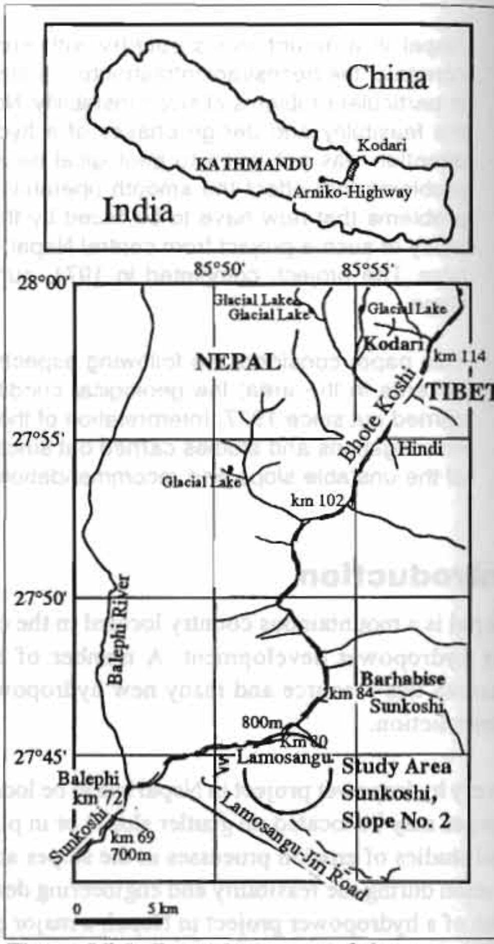

Figure 15.1: Location map of the Bhotekoshi catchment and the Sunkoshi hydropower

The major natural disasters that have affected the Sunkoshi Power Station area since the utility was completed in 1971 are listed below.

- 1976 – a debris flow at Slope No. 2 of the Sunkoshi powerhouse, destroyed the power canal at the toe of the slope and disrupted power generation for many months.
- 1981 – a high intensity flood was caused in the Bhotekoshi by the outburst of the Zhanzangho Glacial Lake in Tibet. It destroyed a number of bridges, a large number of houses, and other property along the Bhotekoshi River, killed four people, and partially damaged the Sunkoshi Hydroelectric Project. The river discharge of the Bhotekoshi at the height of the flood was estimated at 3300 cumecs.
- 1982 – the damming of the Balephi Khola near Phalamesangu caused a high flood in the Bhotekoshi which killed 114 people and swept away 15 houses. It also damaged the power station – it tore away the steel lining of the dam and filled the turbine pits of the powerhouse with mud and debris.
- 1986 – a glacial lake outburst flood in the Sunkoshi caused large-scale damage to the power station.

- 1995 – a debris flow occurred on Slope No. 2 of the Sunkoshi powerhouse, causing extensive damage.
- 1996 – an intensive debris flow in the Larcha Khola tributary of the Bhotekoshi near Tatopani killed 54 people, and swept away 18 houses and an RCC bridge on the main highway. A number of very large boulders, some estimated to weigh more than 1,000 tonnes, destroyed the bridge on the highway (Figure 15.2).

Figure 15.2: **The debris deposit brought down by the Larcha Khola in 1996, a tributary of the Bhotekoshi near Tatopani village. Some of the larger boulders seen in the photograph weigh over 1000 tonnes**

The event of July 5 1995

A large failure occurred in Slope No. 2 of the Sunkoshi Power Station area in July 1995, when the slope was already being investigated in detail (see below), which caused extensive damage to the power project and surrounding property. The mass wasting process started early in the afternoon of July 5, when a great amount of debris gushed down-slope together with a torrent of water, breaching the sides of check dam No. 1 which was located underneath the toe of the upper unstable area. This event was probably caused by a great amount of colluvial material being saturated and loosened during three days of intensive rainfall. This created a torrent of water that ran down from the upper mountain face and drained onto the unstable parts of Block C.

The debris torrent buried the ground floor of a two-storey house adjacent to check dam No. 3. Fortunately, the house was not inhabited at the time. Another 14 houses on the slope were affected. The standing crop was destroyed over a few hundred square metres. Check dams 6, 7, and 8 on the lower elevation of the slope were completely filled up; check dams 1 to 8 were breached from both ends; and check dam 6 was also breached in the middle.

This was the second event of this type since the completion of the hydroelectric project in 1971; the first one occurred in 1976. The recurrence of this danger remains a major threat to the project.

Previous investigations

Instabilities in Slope No. 2 are recognised as the most serious local threat to power generation at the Sunkoshi project. The general plan of Slope No. 2 and surroundings is shown in Figure 15.3, and a general view in Figure 15.4. Slope No. 2 is west-facing. It stretches from an elevation of about 790m up to almost 1,100m (Figure 15.3). It is about 630m long and the average slope angle is 25.5 degrees. The slope angle is gentler in the middle and steepest at the top. The middle part of the slope is terraced and is cultivated (Figure 15.4), some parts are covered with natural vegetation. Some of the lower parts of the slope were previously cultivated for rice paddy but this was stopped by the project because of the instability problems. The upper part of the slope was previously used to grow corn and millet but this area is now covered with landslide debris. The groundwater table varies from about 29.5m in the dry season to about 10m in the wet season. The highest water levels are observed in August and September.

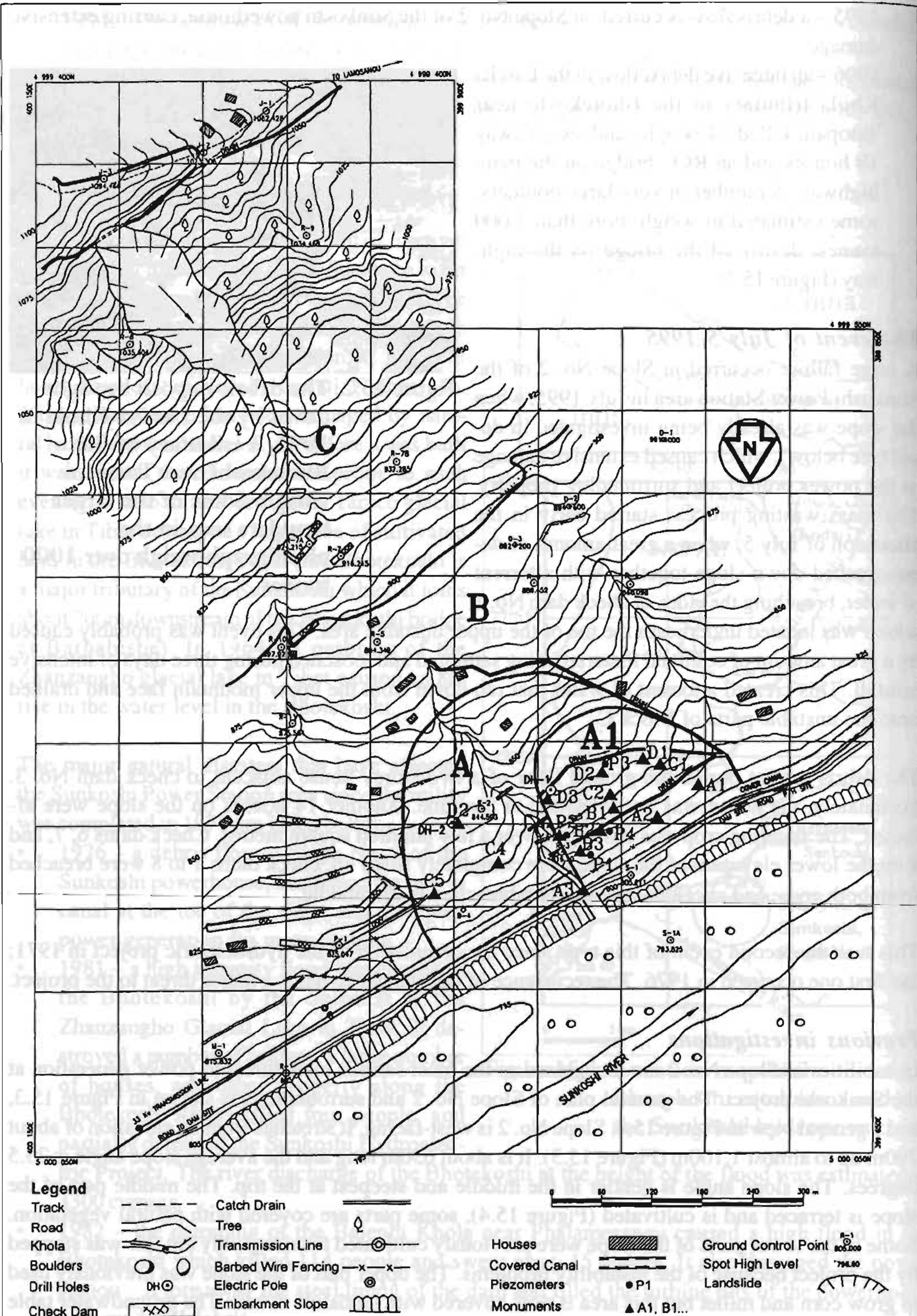

Figure 15.3: General plan of Slope No. 2 and its surroundings

Figure 15.4: **General view of Slope No. 2 towards the south**

Figure 15.5: **Debris accumulation at the check dams brought down by the debris torrent of July 1995**

Slope No. 2 was rated as unstable before the project was completed. The first major impact was the 1976 debris torrent, which caused extensive damage to the power project by breaching the power canal around the toe of the slope. The debris flowed along a gully down the middle of Slope No. 2. To try and mitigate this problem, a series of check dams (numbered from the top part of the slope) were constructed across, and stone masonry walls along, this flow channel (Figure 15.5). These walls subsequently moved as much as 25 cm (Figure 15.6) as a result of movement of the slope.

Figure 15.6: **Displacement of the drainage masonry wall at the toe of the slope**

In 1977-78 a team of geologists from the Water and Energy Resources Development Project (WERDP) of the Electricity Department of the Ministry of Water Resources, studied the slope. The team recommended that four piezometers be installed in the lower and middle parts of the slope to monitor the groundwater table. The piezometer standpipes were installed in 1979 in the lower and middle parts of Slope No. 2. The drill holes were terminated in the colluvium. The standpipes were numbered from P1 to P4 (Figure 15.3) and were at the elevations shown in Table 15.1.

Table 15.1: Elevation of piezometer stand pipes

Piezometer No.	Elevation, m	Depth, m
P1	807.850	11.35
P2	817.050	14.20
P3	839.200	16.00
P4	809.000	8.80

Piezometer P2 became clogged at the very beginning, whilst piezometer P3 remained dry for the whole period of monitoring. Piezometers P1 and P4 remained mostly dry and the water table rose above the bottom only during the wet season. Piezometer P1, located at the bottom part of the slope, recorded the highest water table on September 5, at 0.47 m above the bottom of the piezometer at an elevation of 796m. Piezometer P4 recorded the maximum water level at 816.2 m on various dates. The maximum water table was recorded around the beginning of September.

Fifteen reference monuments marked as A1, A2, B1, C1, D1, and so on, were installed to monitor movement at different parts of the slope (Figure 15.3). Monitoring of these monuments over 14 years

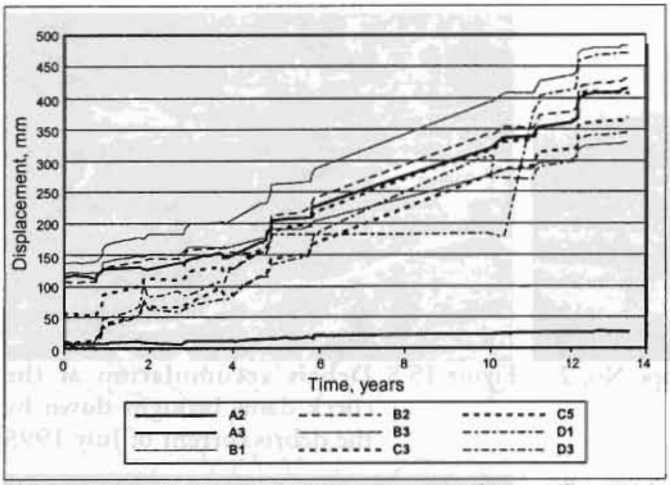

Figure 15.7: **Horizontal displacement of the reference monuments against time No axis labels, still to come**

has shown total displacements varying from 0.09 m at A1 to 1.32 m at B1. The relation between horizontal displacement and time is illustrated in Figure 15.7.

The water level in the piezometers rose in the wet season; horizontal displacement of the slopes took place at the same time. This suggests a close relationship between the rise in the groundwater table and the horizontal displacement of the reference monuments.

The information obtained from these investigations was used to establish a monitoring programme for the slope. However, the core logs from drilling for the piezometers did not provide adequate information on the quality of the slope material and it was difficult to establish the reasons for the instability of the slope from the information provided by the investigations carried out between 1977 and 1990.

Investigations by the Soil, Rock and Concrete Laboratory

In 1990, NEA's Soil Rock and Concrete (SRC) Laboratory, was entrusted with studying Slope No. 2. The laboratory studied the slope with the aim of trying to formulate a permanent solution and devise measures to stabilise the slope. The SRC was assisted by teams from the Japanese International Cooperation Agency (JICA) and HMGN's Water Induced Disaster Prevention Technical Centre (DPTC) who made field visits and offered valuable advice on the sequence of investigation. The team of engineers formed by NEA's Design Department to study the slope started work in 1990. The investigations were designed to answer the following questions.

- Is there just one distinctive instability block or are there a number of smaller blocks?
- What are the causes of the mass erosion processes?
- What immediate and short-term measures are required for their control?
- What is the long-term solution for stabilising the slope?

The results of the various investigations are described in detail in the following.

Geological conditions

Figure 15.8 shows the geological map of the area and Figure 15.9 the structural map. The bedrock under Slope No. 2 is composed of rocks of the Midland meta-sediment group or Kuncha Formation consisting of phyllite, quartzose-phyllite, meta sandstone and grey pellitic quartzite (Maruo et al. 1993). Structurally, the phyllite rocks constitute the core of the Lamosangu anticilinorium (Department of Mines and Geology 1985).

The unstable part of Slope No. 2 is entirely composed of colluvium, which is made up of fragments of phyllites of various sizes and shapes in different states of weathering. The finer material is represented by silt and sand size particles derived from the weathering of phyllites. This soil is

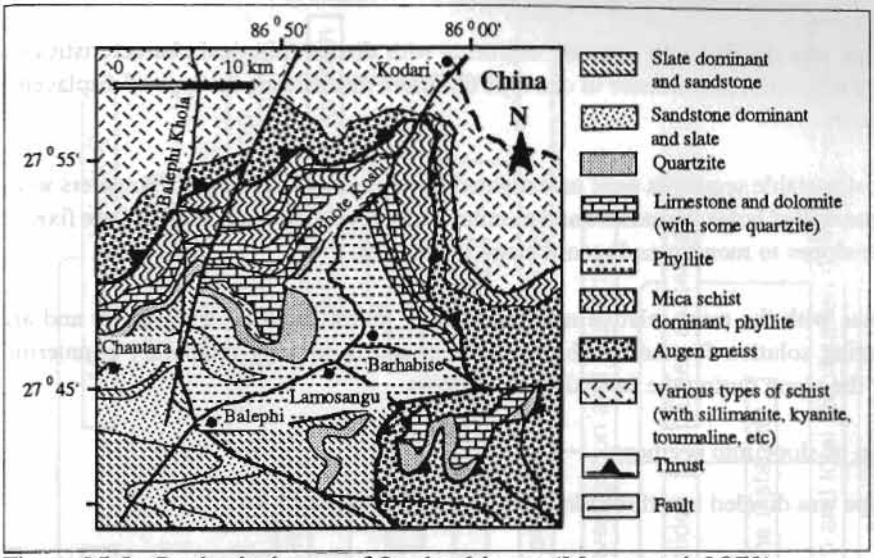

Figure 15.8: **Geological map of Sunkoshi area** (Maruo et al. 1973)

greatly affected by the seasonal rise of the groundwater table in the monsoon. The rise in the water table not only lubricates the slip surface but also causes the shear strength of the soil to decrease resulting in a decrease in slope stability.

The properties of the soil of Slope No. 2 have not been studied because of the problems of soil sampling in non-cohesive (granular) material; using present-day techniques it is difficult to obtain a reasonable quality sample at a reasonable cost. Use of the Standard Penetration Test (SPT) and Dynamic Cone Penetration Test (DCPT) methods to evaluate the strength properties of the soil formation was restricted by the presence of large-size fractions in the colluvium.

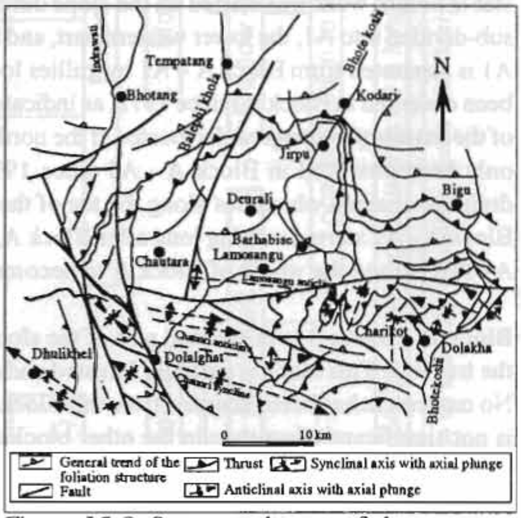

Figure 15.9: **Structural map of the Sunkoshi area** (JICA 1985)

Investigations to identify unstable areas

Plan

The investigations were designed to discover whether the instabilities located at the top of the slope and the landslide at the bottom were one interrelated phenomenon or separate unrelated processes on the same slope, and whether they were related to the rise in the water table in the slope. Permanent counter-measures would be designed once the size of the instability was known.

The logical diagram used to identify which areas of Slope 2 were unstable is presented in Figure 15.10. The planned approach for identifying the unstable areas of Slope No. 2 was as follows.

The slope was divided into separate segments with distinct physical characteristics such as the presence of gullies, prominence of one type of failure mechanism, the type of displacement, or the topography.

The most unstable segments were investigated by exploratory drilling. Piezometers were installed inside the drilled holes to measure and monitor water levels. Reference piles were fixed in rows all over the slopes to monitor and record slope movement.

The areas with the most relative movement were investigated in detail to try and arrive at an engineering solution for the instability problem and to identify temporary countermeasures to protect the slope during the investigation process.

Division of slope into segments

The slope was divided into three blocks A, B, and C (Figure 15.3).

Block A – Block A is the area of an old landslide at the lower end of the slope. This area had been stable before work was started on the slope during construction of the power station. Block A was sub-divided into A1, the lower western part, and the remainder, called A minus A1 or A - A1. Block A1 is separated from Block A – A1 by gullies located on either side of the slope. Movements have been observed in Block A1 since 1972, as indicated by the horizontal displacement (by about 25 cm) of the masonry drainage walls located at the northern end of the block (Figure 15.6). Movement has only been observed in Block A - A1 since 1992 in the form of (progressing) cracks along the drainage channel which lies along the toe of the slope between the slope and the power canal. As Block A - A1 started moving long after Block A, it seems likely that it was the movement of Block A1 that caused the whole of Block A to become unstable.

Block B – Block B is the central part of the slope. It is located above Block A and stretches up to the tree line. This block is partially forested and covered by thick vegetation, and partly cultivated. No movement has been recorded from this block. It is relatively stable, even though the slope angle is not significantly less than in the other blocks.

Block C – Block C is the uppermost and steepest part of the slope and is separated from the middle by a line of natural vegetation. In the past, this block comprised a number of small, superficial instabilities (mass wasting processes) and was partly used to grow corn and millet. A large part of this block is under natural vegetation. This part of the slope contributed a large quantity of debris to the 1976 monsoon debris flow and the debris torrent of July 1995. At present, it contains two increasingly unstable areas.

Investigations and Monitoring

A seismic profile of the slope was made in 1991 (Figure 15.11). The first stability analysis was carried out using the results of seismic refraction.

At the end of December 1994 the slope was investigated by exploratory drilling; two holes were drilled to a depth of 36m at the top of blocks A1 and A-A1 as marked on Figure 15.3. Piezometers were installed in each of these holes. Two holes were drilled to a depth of 36m at the top of Block A1. It is planned to drill a third hole in Block B. Then reinforced concrete (RCC) piles were installed in rows

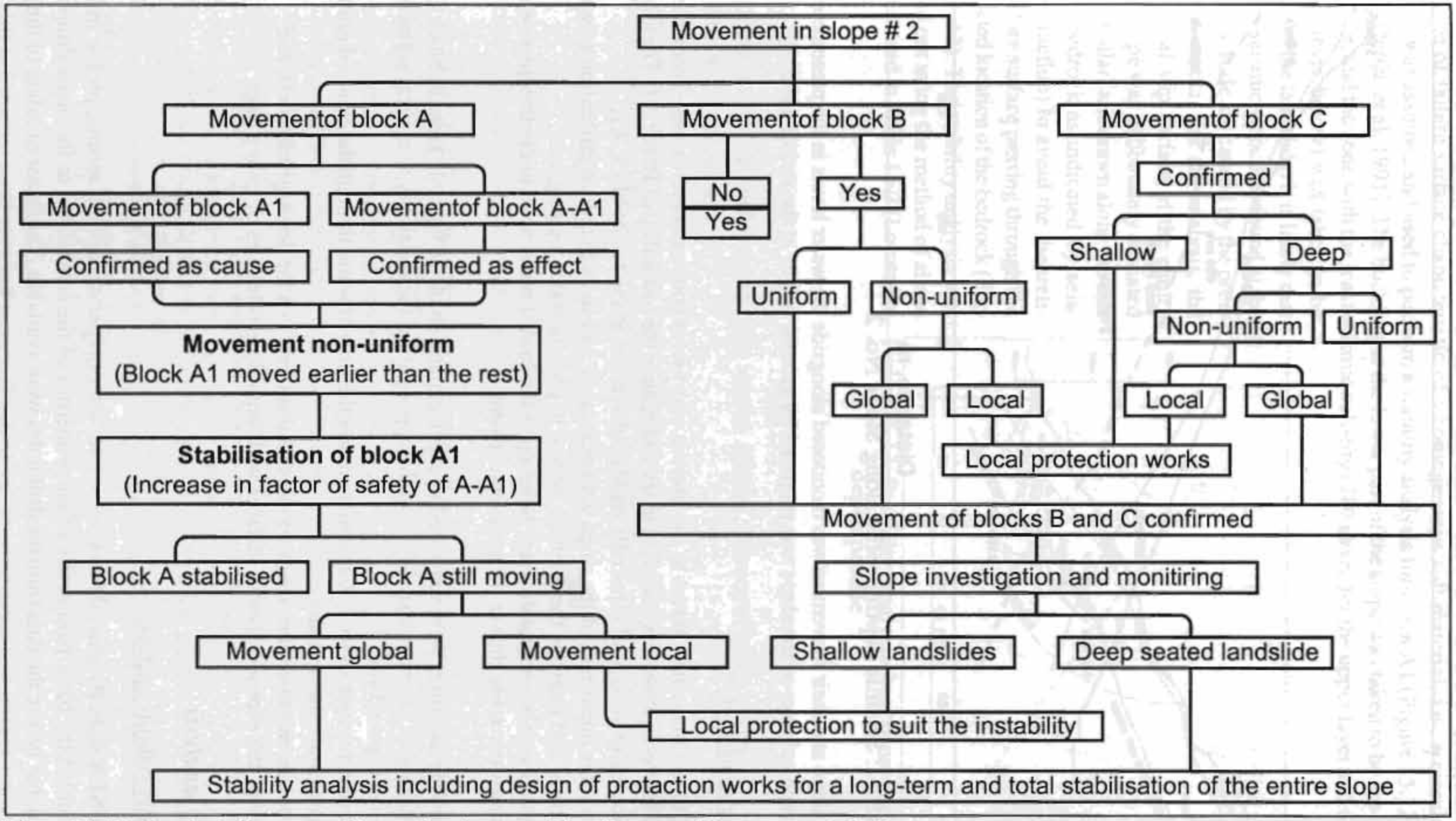

Figure 15.10: **Logical diagram of investigations to identify unstable areas and design countermeasures**

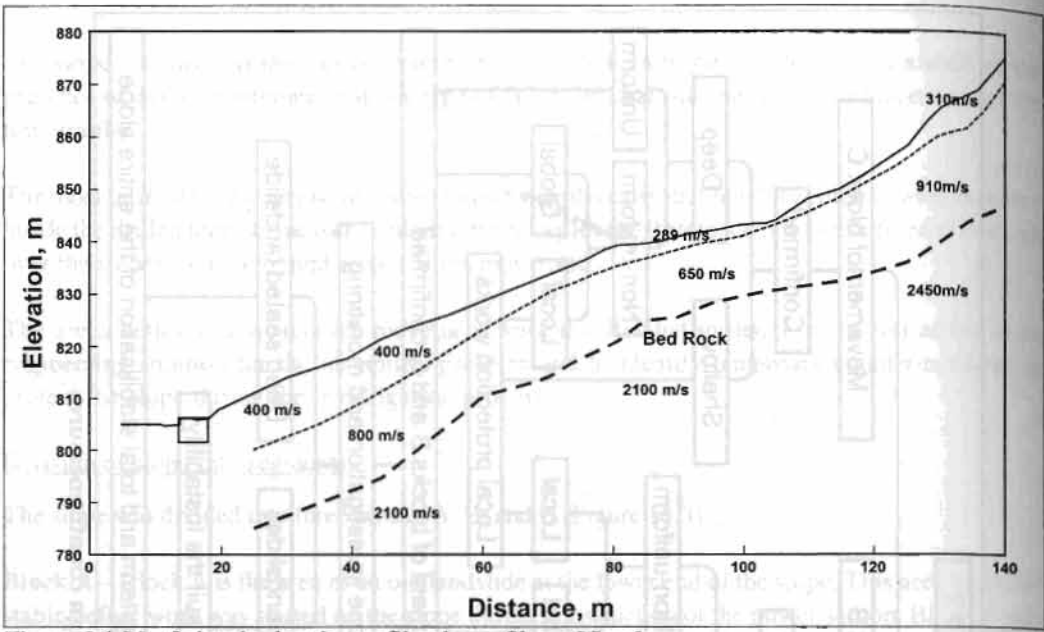

Figure 15.11: **Seismic depth profile along Slope No. 2**

over the slope and their movement was monitored alongside the water levels in the piezometers. A topographical map of the slope was prepared by ground survey at the end of 1995.

Temporary measures

Because of the immediate threat to the project, short-term countermeasures were recommended before the investigation was complete to try and reduce the instability of Block A1. These were

- to stop cultivation, and especially paddy cultivation, at the top of block A1;
- to treat the upper part of the slope with red clayey soil so as to reduce infiltration of water;
- to extend and improve the drainage system to prevent water logging; and
- to install five horizontal drainage holes up to the lowest water level to control the rise in the groundwater table during the monsoon season.

The following measures were suggested to check expansion of the unstable areas in block C:

- to construct a drainage channel along the upper part of the instability to prevent surface flow into the exposed soil;
- to design a system of RCC drains to minimise the flow of water through the exposed ground in order to minimise soil loss;
- to implement bio-engineering measures in areas between the drainage channels; and
- to cover the exposed ground surfaces with suitable geo-textiles or gunny bags.

Stability analysis

Preliminary stability analysis

The first NEA stability analysis was carried out after preparation of the seismic profile in 1991, which enabled the basic parameters of the properties of the soil related to the instabilities to be identified, but before the data from the drill holes were available. The factor of safety of the slope during the dry season was taken to be '1' as no displacement has ever been recorded at this time.

The type of failure surface characteristic of a homogeneous soft material, i.e., a circular failure surface, was assumed and used to perform a stability analysis for block A1 (Figure 15.12 and Box 15.1) (Deoja, et al. 1991). The buckling at the lower part of the slope was taken to be the toe of the landslide, and the zone with the least seismic velocity (280 m/sec for the upper layer and 650 m/sec for the layer below) was taken to be the top of the landslide. It is likely that the low seismic velocities found at the top of the slide are caused by the presence of cracks. For the analysis, the theoretical slip surface at the centre of the slope was deliberately deviated from circular (and drawn along the line of the bedrock as indicated by seismic refraction) to avoid the theoretical failure surface passing through the calculated location of the bedrock (Figure 15.12). The stability analysis was carried out using the method of slices as presented in Table 15.2 (Lomtadze 1977).

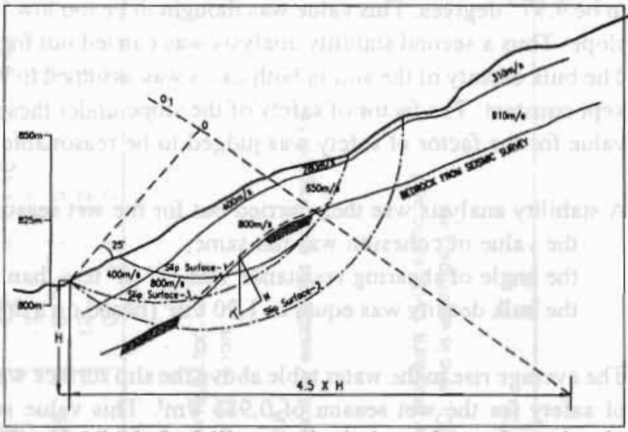

Figure 15.12: Stability analysis based on the seismic depth profile

Box 15.1

Method used to determine the most likely (theoretical) path of the slip surface

The graphical method (Fellenious method) was used to draw the theoretical slip surface. The centre of the slip surface is drawn as follows. The steps are illustrated in Figure 15.12.

- An angle of 25 degrees was added to the slope and a line drawn
- An angle of 35 degrees was added to the upper surface of the slope and a second line drawn (Values taken from tables in Lomtadze (1977))
- The meeting point of these two lines was taken to be one of the centres of the slip surface (marked O).Other probable centres are located along the line 0-01 passing through the point 0 and a second point located one height (of the slope) below and 4.5 height (of the slope) along the horizontal into the slope from the toe
- Circles were drawn from point 0 as well as other centres located along the line 0-01 to obtain a slip surface passing through the toe of the slope, where slope movement is observed, and the top of the slope, characterised by the least velocity of seismic waves. Circles (theoretical slip surfaces) drawn from centres including the point 0 were either cut very deep into the bedrock (not possible) or deviated considerably either at the toe or at the top of the slope. Of all the probable centres, 01 was the best fit for a slip surface passing through both the toe and the top of the slope. However, this theoretical slip surface cut the bedrock within the range of high weathering (about 10m).Thus the circular path of the curve was deliberately changed and drawn 'free hand' along the top of the bedrock. The area included within this arc was subjected to stability analysis.

A stability analysis was carried out for the dry season. The first stability analysis was based on the assumption that the slope has a factor of safety of one during the dry season. The value of cohesion was assumed to be 0.25 t/m^2 for the lower six slices and zero for the remaining three slices (effect of loosening and loss of fines by piping from the upper part of the slope). From this analysis, the angle of shearing resistance (φ)of the material composing the slope was determined to be 9.97° degrees. This value was thought to be too low for the type of colluvium composing the slope. Thus a second stability analysis was carried out for an angle of shearing resistance of 20°. The bulk density of the soil in both cases was assumed to be 1.75 t/m^3. The value of cohesion was kept constant. The factor of safety of the slope under these conditions was found to be 1.48. This value for the factor of safety was judged to be reasonable during the dry season.

A stability analysis was then carried out for the wet season. For this it was further assumed that

- the value of cohesion was the same;
- the angle of shearing resistance was 18° (2° less than in dry conditions); and
- the bulk density was equal to 1.90 t/m^3 (based on a dry bulk density of 1.75 t/m^3).

The average rise in the water table above the slip surface was equal to 11m giving an average factor of safety for the wet season of 0.985 t/m^3. This value seems reasonable as the slope is fairly unstable having shown a maximum displacement of 1.32m (pillar C1) and an average horizontal displacement of 1.056m over 14 years. The rate of horizontal displacement of the slope appears to be constant at about 7-10 cm per year.

Final stability analysis

The final stability analysis was performed in 1996 after the data from the drill holes became available. Drill hole DH 1 was located at almost the same position as the seismic refraction line.

The drill hole data showed that the assumptions made on the basis of the seismic survey were not completely correct. At the drill hole altitude of 804.5m, the bedrock was actually located at a depth of 34.50m and not 15.10m as indicated by the seismic refraction. Furthermore, an accumulation of clay at a depth of 31m indicated the location of the possible slip surface. This level accurately matches with the slip surface originally plotted in the preliminary stability analysis on the basis of the seismic profile, before the erroneous correction was made for the calculated position of the bedrock.

At an elevation of 809.50m, the groundwater table is located at 29.50m (minimum level recorded in the dry season.

Separate stability analyses were performed for blocks A1 and (A-A1). The analysis for A1 was carried out using both the graphical method with a circular slip surface (Figure 15.13) and the Hoek and Bray method. The stability analysis for A-A1 was carried out using the Hoek and Bray method only.

The stability analysis for Block A1 using the graphical method is presented in detail in Table 3; the graphical plot is shown in Figure 15.13. As with the preliminary stability analysis, the soil properties were taken to be : (Φ) = 20 degrees for the lower part of the slope decreasing step by step in the upper sections (Table 15.3) ; cohesion (c)= 0.25 t/m^2 ; dry density (D_d) = 1.75 t/m^3 ; wet density (D_w) = 1.9 t/m^3 ; rise in water table during the wet season = 19.5 m ; decrease in the Φ- value of the soil upon wetting = 10%.

The factor of safety was found to be approximately equal to 1.1 in dry conditions, close to a state of equilibrium, and to decrease to 0.89 as the groundwater table rises in the wet season.

Table 15.2: **Slope stability analysis on the basis of seismic refraction**

Parameter	Slice									Sum
	1	2	3	4	5	6	7	8	9	
Area of slice, m^2	0.63	3.6	5.6	6.8	8	8	7	5.6	2.3	
Thickness of slice, m	1	1	1	1	1	1	1	1	1	
Density (dry) of Slice, t/m^3	1.75	1.75	1.75	1.75	1.75	1.75	1.75	1.75	1.75	
Weight of slice, ton (W)	1.1025	6.3	9.8	11.9	14	14	12.25	9.8	4.025	83.1775
A, deg	-15	-8	0	9.5	18	24	36	47	60	
Sin A	-0.259	-0.139	0	0.165	0.309	0.407	0.588	0.731	0.866	
Cos A	0.966	0.99	1	0.986	0.951	0.913	0.809	0.682	0.5	
W Cos A, ton	1.07	6.24	9.8	11.73	13.31	12.73	9.91	6.68	2.01	73.48
W Sin A, ton	-0.29	-0.88	0	1.96	4.33	5.7	7.2	7.16	3.49	28.67
Φ	?	?	?	?	?	?	?	?	?	
Cohesion (c), t/m^2	0.25	0.25	0.25	0.25	0.25	0.25	0	0	0	1.5
Length of Slip Surface (L), m	3	12	12	12	12	12	12	12	12	99
cL	0.75	3	3	3	3	3	0	0	0	15.75

'A' is the angle between the normal and the resisting component of the force.

In Dry Season
Summation of W Cos A =73.54 ton
Summation of W Sin A = 28.63 ton

In wet season
Summation of W Cos A =79.84 ton
Summation of W Sin A = 31.14 ton

Factor of Safety, F = **[Summation of W Cos A x tan Φ + cL]/Summation of W Sin A**

For the State of Equilibrium for F = **1, Φ = 9.97 deg**, which is low for colluvium composed of moderately weathered rock fragments

Hence, second analysis is carried out for the value of Φ = 20 deg.
For Φ = 20 deg., the Factor of Safety of the Slope = 1.48

The reduction in the Factor of Safety (F) in the wet season is caused mainly by the increase in pore water pressure, hydrostatic and hydrodynamic forces as well as increases in the weight of the material acting against the resisting force (D), and is estimated as:

F = [Summation of W Cos A x tan Φ + cL-D]/Summation of W Sin A
For a Creep, Factor of Safety F = 1, D = 9

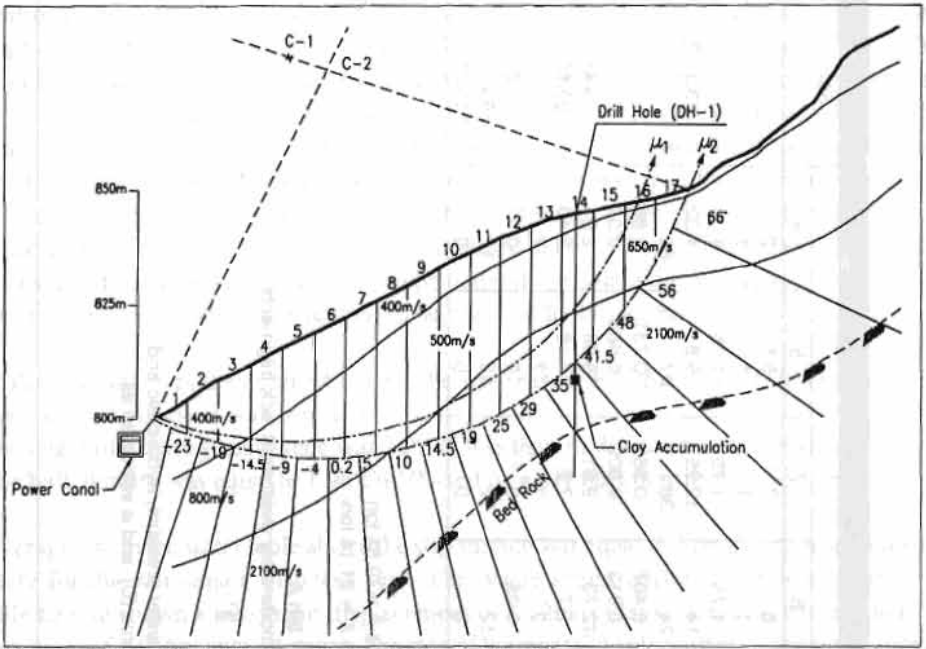

Figure 15.13: **Stability analysis of Slope No. 2**

A second analysis of A1 was carried out using the Hoek and Bray method, which can be used for stability analysis of a slope composed of homogeneous material. The material properties were assumed to be: angle of shearing resistance, Ø = 20°; cohesion c = 0.25 t/m²

Using this method, the factor of safety under dry conditions was calculated to be 1.08.

The factor of safety in the wet season was calculated as follows. The lowering of the factor of safety during the monsoon was assumed to be mainly due to a decrease in the values of cohesion c and the angle of shearing resistance (Ø) as a result of the wetting of the soil mass, and of a decrease in stability due to a rise in the piezometric head. The impact of the increase in weight of soil due to wetting was ignored because of the absence of relevant data.

The factor of safety F in the wet season was calculated using the following.

Dimensionless Factor = c/(DH tan Ø) = 0.25x75/(1.6x35xtan15) = 0.1

where D = bulk density of the soil in t/m³

H = height of the slope, m

Ø = value of the angle of shearing resistance of the soil, degrees

Using this dimensionless factor, the slope angle of 30 degrees and the slope height of 35m, the Factor of Safety (F) is calculated from

c/(DHF)=0.042

giving

F = 0.6 for wet season conditions.

Table 15.3: Final slope stability analysis

Parameter	Slice																	
	1	2	3	4	5	6	7	8	9	10	11	12	13	14	15	16	17	Sum
Area, sq. m.	32	97	151	193	235	270	296	319	329	347	368	355	335	304	251	180	71	4133
Thickness, m	1	1	1	1	1	1	1	1	1	1	1	1	1	1	1	1	1	
Density (dry)	1.75	1.75	1.75	1.75	1.75	1.75	1.75	1.75	1.75	1.75	1.75	1.75	1.75	1.75	1.75	1.75	1.75	
W, ton	56	169.75	264.25	337.75	411.25	472.5	518	558.25	575.75	607.25	644	621.3	586.25	532	439.25	315	124.25	7232.75
A, deg.	-23	-19	-14.5	-9	-4	0.2	5	10	14.5	19	25	29	35	41.5	48	56	66	
Sin A	-0.391	-0.325	-0.25	-0.156	-0.07	0.003	0.087	0.174	0.25	0.325	0.423	0.485	0.574	0.663	0.743	0.829	0.913	
Cos A	0.921	0.945	0.968	0.988	0.998	0.999	0.996	0.985	0.968	0.946	0.906	0.875	0.819	0.749	0.669	0.559	0.407	
W cos A	51.58	160.41	255.79	333.7	410.43	472.03	515.93	549.88	557.33	574.46	583.46	543.6	480.14	398.47	293.86	176.09	50.57	6407.72
W Sin A	-21.9	-56.17	-66.06	-52.69	-28.79	1.42	45.07	97.14	143.94	197.36	272.41	301.3	336.51	352.72	326.36	261.14	113.44	2223.21
	20	20	20	20	20	20	20	20	20	20	18	17	16	15	14	12	10	
Tan Φ	0.364	0.364	0.364	0.364	0.364	0.364	0.364	0.364	0.364	0.364	0.325	0.306	0.287	0.268	0.149	0.212	0.176	
W Cos tan Φ	18.77	58.391	93.109	121.47	149.4	171.82	187.8	200.15	202.87	209.1	189.63	166.3	137.8	106.79	43.785	37.33	8.9003	2103.46
c, t/sq. m	0.25	0.25	0.25	0.25	0.25	0.25	0.25	0.25	0.25	0.25	0.26	0	0	0	0	0	0	
L, m	3	12	12	12	12	12	12	12	12	12	12	12	12	12	12	12	12	195
CL	0.75	3	3	3	3	3	3	3	3	3	3	0	0	0	0	0	0	30.75
D	9	9	9	9	9	9	9	9	9	9	9	9	9	9	9	9	9	

Factor of Safety in dry conditions, Fd = (summation (W Cos A)x tanO +cL)/Summation (W SinA)
or, Fd = (2103.4+30.8)/2224.2 or, Fd= 0.96

Reduction in the Factor of Safety (F) during the wet season is mainly attributed to an increase in the soil density, a decrease in the Φ value, increase in pore water pressure , and hydrodynamic pressure caused by a to rise in the groundwater table.
It is assumed that the value of the angle of shear resistance of the material will decrease by 10% upon wetting.

The factor of safety in the wet season, F_w = 0.83

The same method and values were used to calculate the factor of safety of block A -A1. The factor of safety was calculated to be 1.04 in the dry season. The slip surface corresponding to this factor of safety was the shallowest of all the possible slip surfaces drawn for the stability analysis of this block and was drawn as passing through the middle part of the slope. In reality, the cracks located along the toe of the slop suggest the presence of another slip surface passing through the toe. Hence, another slip surface was plotted passing through the wash out zone (located at a depth of 31m). The factor of safety for this slip surface was calculated to be 0.46 in the wet season.

Conclusions and Recommendations

The studies of Slope No. 2 showed that the movements of Blocks A - A1 and A1 are separate phenomena. They were initiated at different times, their failure mechanisms are different, and they are behaving as separate instabilities. Block B seems to be stable as no movement has been recorded from that slope segment.

Block C contains two progressively increasing superficial instabilities. The upper part of the slope above the larger of the instabilities has numerous tension cracks, which may develop into a circular slip surface.

There is no evidence to suggest that the instability of Slope No. 2 is a single phenomenon affecting the entire slope, rather it seems that the slope is composed of a number of localised instabilities in blocks A and C. The recommendation was made to treat each of these instabilities individually. The individual treatments are listed below. Some were the same as recommended initially, some were new.

- For Block A1
  - Stop cultivation and especially paddy cultivation at the top of Block A1. This has already happened and has resulted in a general decrease in the horizontal displacement rate of the slope.
  - Treat the upper part of the slope with red clayey soil so as to prevent infiltration of water into the slope.
  - Extend the drainage system of this part of the slope to prevent water logging and drill five horizontal drainage holes up to the lowest water level to control the rise in the groundwater table.
  - Apply bio-engineering to prevent or control soil loss.
  - Continue to monitor the movement of each block as stabilisation of block A1 may lead to stabilisation of A-A1.

- For Block C
  - Construct a drainage channel along the upper part of the instability to prevent surface flow into the exposed soil of the instability.
  - Design a system of RCC drains to prevent water flowing through the ground and thus prevent soil loss.
  - Carry out bio-engineering in areas between the drainage channels.
  - Cover the exposed surface of the ground with either a suitable geo-textile or with gunny bags.
  - Cover and fill the tension cracks in the vicinity of the instabilities with red clay to prevent infiltration of water into the cracks.

- Construct a retaining wall with horizontal drains along the upper part of the landslide to control slumping ofsoil mass weakened by moisture during the wet season.

References

Department of Mines and Geology (1985) *Geological Map of Nepal*. Kathmandu: HMG/Nepal

Deoja, B.; Dhital, M.R.; Thapa, A.; Wagner, A. (eds) (1991) *Mountain Risk Engineering Handbook, Parts 1 and 2*. Kathmandu: ICIMOD

ITECO Engineering (1996) *Hazard Mitigation in Northern Sunkoshi and Bhote Koshi Water Catchment areas*. Kathmandu: Department of Roads/HMG

Lomtadze, V.D. (1977) *Engineering Geology*. Nedra: Engineering Geodynamics

Maruo Y.; Ohta, Y.; Akiba, C.; Arita, K. (1993) 'Chautara Region'. In Hashimoto, S., Ohta, Y. and Akiba, C, (eds) *Geology of the Nepal Himalayas*, pp 69-97. Sapporo: Himalayan Committee of University and Saikon Publishing Co. Ltd

JICA (1985) *Master Plan Study on the Koshi River Basin, Water Resources Development*, Final Report, Vol. 2. Kathmandu: Japan International Cooperation Agency (JICA)